

Edge Detection Algorithm Inspired by Pattern Formation Processes of Reaction-Diffusion Systems

Atsushi Nomura, Makoto Ichikawa, Koichi Okada, Hidetoshi Miike and Tatsunari Sakurai

Abstract—This paper presents a quick review of reaction-diffusion systems and the application of a discretized version of a reaction-diffusion system to edge detection in image processing. A reaction-diffusion system refers to a system consisting of diffusion processes coupled with reaction processes. Several reaction-diffusion systems exhibit pattern formation processes, in which the systems self-organize spatio-temporal patterns of target and spiral waves propagating in two-dimensional space. In addition, some of the systems having strong inhibitory diffusion self-organize stationary patterns; the Turing pattern is one of the typical examples of the stationary patterns observed in reaction-diffusion systems under strong inhibitory diffusion. We have previously found that the discretized version with strong inhibition has a mechanism detecting edges from an image intensity distribution. The mechanism divides an image intensity distribution into brighter or darker intensity areas with a threshold level, and organizes pulses along edges of the divided areas. By searching an output distribution of the version for pulses, we can achieve edge detection. However, since the threshold level is usually fixed at a constant value in the version, the mechanism is not applicable to gray level images. Thus, this paper furthermore proposes an edge detection algorithm consisting of two pairs of the version with a variable threshold level. We apply the edge detection algorithm and a representative algorithm proposed by Canny to several artificial and real images in order to confirm their performance.

Index Terms—Reaction-diffusion, pattern formation, pattern recognition, strong inhibition, edge detection, non-linear reaction, Turing pattern, FitzHugh-Nagumo

I. INTRODUCTION

REACTION-DIFFUSION systems exhibit pattern formation processes, in which they self-organize spatio-temporal patterns such as target and spiral waves propagating in space. The Belousov-Zhabotinsky reaction system [1], [2] known as a chemical reaction system is a representative example of the reaction-diffusion systems. Particular points on the two-dimensional chemical reaction system behave as non-linear oscillators of a chemical reaction. Simultaneously, chemical substances generated by the chemical reaction diffuse into neighboring regions, in which the diffused substances again trigger non-linear oscillators of the chemical reaction. Thus, the chemical reaction system self-organizes chemical waves propagating in space. The reaction-diffusion systems including the Belousov-Zhabotinsky reaction system are well studied as diffusion processes coupled with non-linear reactions. Reaction-diffusion systems widely exist and

self-organize spatio-temporal patterns also in other natural systems [3].

A set of reaction-diffusion equations describes pattern formation processes observed in a reaction-diffusion system. The reaction-diffusion equations consist of diffusion equations coupled with reaction terms describing a non-linear oscillator. For example, Keener and Tyson proposed a pair of reaction-diffusion equations for modeling a pattern formation process observed in the two-dimensional Belousov-Zhabotinsky reaction system [4]. The equations have two variables named activator and inhibitor, which respectively activates and inhibits the chemical reaction. Since the activator usually diffuses more rapidly than or equally to the inhibitor in the reaction system, the diffusion process of the activator drives propagation of target and spiral waves.

The strong inhibition prevents the propagation of waves and induces stationary patterns of periodic waves. In the Belousov-Zhabotinsky reaction system an activator substance usually diffuses more rapidly than an inhibitor one. Castets et al. [5] and Kepper et al. [6] found that a chemical reaction system exhibits rapid inhibitory diffusion in comparison to activator's diffusion and successfully realized stationary periodic waves in real laboratory experiments. We also found stationary patterns by adding the strong inhibitory diffusion to the Oregonator model of the chemical reaction system in numerical experiments [7].

Turing had predicted the existence of stationary periodic waves induced by strong inhibitory diffusion in reaction-diffusion systems in his theoretical paper [8]. A diffusion process generally brings a uniform distribution of a substance. However, Turing presented a scenario in which strong inhibitory diffusion causes instability on a uniform distribution and stable stationary patterns appear. The Turing pattern refers to stable stationary waves induced by the Turing scenario. Gierer and Meinhardt accepted the Turing scenario and proposed more realistic reaction-diffusion equations with strong inhibitory diffusion, in order to understand biological pattern formation processes [9]. The equations successfully realized regeneration of a head of Hydra and grafting a head section to another terminal section of its body in numerical experiments. More recent evidence found in biological systems supports the Turing scenario [10]; biologists have accepted the realistic reaction-diffusion equations as a mathematical model of pattern formation processes observed in biological systems [11]. The key point of the scenario is the strong inhibitory diffusion.

If turning our attention to pattern recognition processes in biological visual systems, we can find several interesting phenomena and their mathematical models. Lateral eyes of *Limulus*, which is a kind of crab, exhibit the Mach bands

This research work was supported in part by a Grant-in-Aid for Scientific Research (C) (No. 20500206) from the Japan Society for the Promotion of Science.

A. Nomura, K. Okada and H. Miike are with the Yamaguchi University, Japan.

M. Ichikawa and T. Sakurai are with the Chiba University, Japan.

effect, which is also found in the human visual system [12]. Previous physiological experiments show that the Mach bands effect is caused by the long-range inhibition in a lateral inhibition mechanism working on outputs of ommatidia, which are individual visual receptor units [13]. A mathematical model taking account of the lateral inhibition mechanism completely simulated the Mach bands effect in the lateral eyes of Limulus [14]. These previous physiological and psychological studies have suggested that the long range inhibition is the key point in understanding pattern recognition processes. The long range inhibition is also understood as the strong inhibitory diffusion in reaction-diffusion systems.

While many researchers were interested in reaction-diffusion systems, Kuhnert et al. presented an interesting idea performing image processing with a reaction-diffusion system [15], [16]. They utilized a light-sensitive Belousov-Zhabotinsky reaction-diffusion system, in which we can control its chemical state and modulate its two-dimensional distribution by illumination light. By projecting an image intensity distribution onto the surface of the two-dimensional chemical reaction system, they demonstrated image pooling, edge enhancement and segmentation on the projected distribution. However, the demonstration including edge enhancement does not appear stationarily, but appear transiently. More recently, Sakurai et al. proposed a method of controlling chemical wave propagation by utilizing illumination light and succeeded in designing a path of the wave propagation [17]. These previous experimental studies have completely linked reaction-diffusion systems with image processing and computer vision research. Adamatzky et al. named a class of nature-inspired computer algorithms utilizing reaction-diffusion systems 'reaction-diffusion algorithm' and presented a novel architecture of reaction-diffusion computers [18].

From an engineering point of view, the Chua's circuit is an interesting topic for reaction-diffusion systems [19]. An individual Chua's circuit behaves as a non-linear oscillator and a resistively coupled Chua's circuit system realizes a reaction-diffusion system. A two-dimensional version of the Chua's circuit also self-organizes spatio-temporal patterns of target and spiral waves as well as the Turing pattern [20]. Reaction-diffusion systems are realizable on circuit systems consisting of the Chua's circuits and have several application areas such as finger-print recognition.

We have proposed several reaction-diffusion algorithms for image processing and computer vision research. A discretized version of the FitzHugh-Nagumo reaction-diffusion equations detects edges and segments from an image intensity distribution provided as an initial condition of the equations [21], [22], [23]. Kurata et al. analyzed a network of discretely coupled oscillators, each of which is described with the FitzHugh-Nagumo ordinary differential equations, and presented a condition required for stable results of edge detection and segmentation [24]. Nomura et al. proposed an algorithm of detecting a stereo disparity map from a pair of stereo images; the stereo algorithm utilizes multiple reaction-diffusion systems exclusively linked [25]. We have imposed strong inhibition on these reaction-diffusion algorithms, as inspired by biological pattern formation processes and as suggested by biological

visual systems.

The present paper proposes a reaction-diffusion algorithm with strong inhibition for edge detection. In contrast to the previous edge enhancement phenomenon reported by Kuhnert et al. [16], the proposed algorithm detects edges by organizing not moving, but stationary pulses. Our previous algorithm utilizing a discretized version of the FitzHugh-Nagumo reaction-diffusion equations detects edges with a fixed threshold level dividing an image intensity distribution into brighter or darker intensity areas [21]. Thus, the previous algorithm is designed not for gray level images, but for binary images. Although our latest reaction-diffusion algorithm of edge detection is designed for gray level images with a variable threshold level [23], there still exists a problem of how to eliminate false pulses, which are by-products in introducing the variable threshold level. In order to solve the problems in the previous reaction-diffusion algorithms, we propose an edge detection algorithm applicable to gray level images with the variable threshold level. By utilizing two pairs of the FitzHugh-Nagumo reaction-diffusion equations, we design the algorithm to eliminate the false pulses. This is the main difference between the proposed algorithm and the latest one [23].

The organization of this paper is as follows. Section II presents a quick review of reaction-diffusion systems and their reaction-diffusion equations, of which a discretized version self-organizes stationary pulses at edge positions. Section III presents a reaction-diffusion algorithm proposed here for edge detection from gray level images. Section IV presents several experimental results for artificial and real images. In particular, the section presents quantitative evaluations on the proposed algorithm in comparison to a previous algorithm proposed by Canny [26]. Finally, Section V concludes this paper with a summary of the proposed algorithm and future work required for the reaction-diffusion algorithm of edge detection.

II. REACTION-DIFFUSION SYSTEMS

A. Diffusion equation and its application to image processing

A diffusion equation describes how much substance or heat spatially spreads, as time proceeds. Let $u(\mathbf{x}, t)$ be a distribution of substance or heat; the distribution u is defined in space $\mathbf{x} \in \mathbf{R}^n$ and at time t . Then, a diffusion equation without a source term becomes

$$\partial_t u = D \nabla^2 u, \quad (1)$$

in which D is a diffusion coefficient, $\partial_t = \partial/\partial t$ and ∇^2 is the Laplacian operator. An initial condition for u is $u(\mathbf{x}, t = 0.0) = U_0(\mathbf{x})$. Hereafter, we define $\mathcal{D}(U_0; D, t)$ as a solution of a diffusion equation having a diffusion coefficient D , an initial condition U_0 and computed until time t . That is

$$\mathcal{D}(U_0; D, t) = u(\mathbf{x}, t) \quad (2)$$

obtained with Eq. (1) and the initial condition U_0 . In other words, $\mathcal{D}(U_0; D, t)$ is a filter for a spatial distribution $U_0(\mathbf{x})$ and its output is the distribution $u(\mathbf{x}, t)$. Indeed, a solution of the diffusion Eq. (1) is a convolution of its initial condition U_0 and a Gaussian function, of which the spatial spread

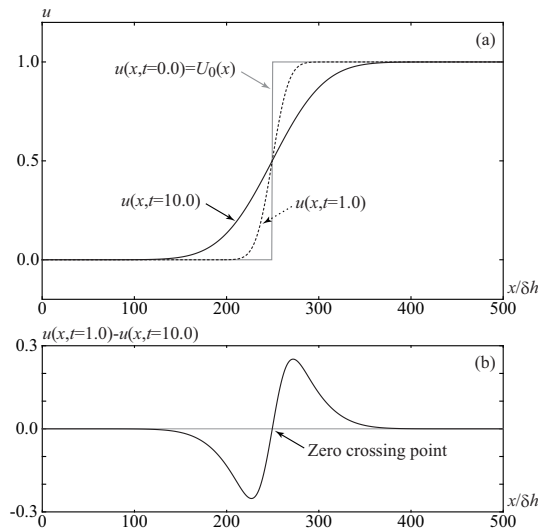


Fig. 1. Difference of two solutions obtained by a diffusion equation $\partial u/\partial t = \nabla^2 u$ at two different time instances. Figure (a) shows the two solutions $u(x, t = 1.0)$ and $u(x, t = 10.0)$; a step-wise distribution $U_0(x)$ was provided for the initial condition $u(x, t = 0.0)$ of the diffusion equation. Figure (b) shows the difference of the two solutions $u(x, t = 1.0) - u(x, t = 10.0)$; a zero-crossing point in the difference is located at the edge position of the initial condition $U_0(x)$. The diffusion equation was discretized and solved with a finite difference δh in space x .

depends on duration of diffusion t and the diffusion coefficient D . Figure 1(a) shows two spatial distributions $\mathcal{D}(U_0; D = 1.0, t = 1.0)$ and $\mathcal{D}(U_0; D = 1.0, t = 10.0)$ for a step-wise distribution $U_0(x)$.

Many image processing algorithms utilize a Gaussian filter for reducing random noise contained in image intensity distributions. For example, Marr and Hildreth proposed an edge detection algorithm with a Laplacian of Gaussian filter; the algorithm reduces random noise with the Gaussian filter and then detects edges by searching an output of the Laplacian of Gaussian filter for zero-crossing points [27]. The difference of excitatory and inhibitory Gaussian filters approximates the Laplacian of Gaussian filter, when the inhibitory Gaussian filter spreads more than the excitatory one. Thus, they imposed the long-range inhibition on the edge detection algorithm.

A diffusion equation brings an alternative edge detection algorithm for the difference of two Gaussian filters proposed by Marr and Hildreth [27]. As mentioned above, a Gaussian filter for an image intensity distribution is equivalent to a solution of a diffusion equation [28], for which the image intensity distribution is provided as its initial condition. Thus, the difference of the two Gaussian filters is equivalent to the difference of two solutions obtained at two different time instances with a single diffusion equation [29], or to the difference of two solutions obtained at a time instance with two diffusion equations having two different diffusion coefficients of strong inhibition and weak excitation [21]. That is, the difference of two Gaussian filters becomes an alternative form such as

$$\mathcal{D}(U_0; D, t_1) - \mathcal{D}(U_0; D, t_2), \quad 0 < t_1 < t_2, \quad (3)$$

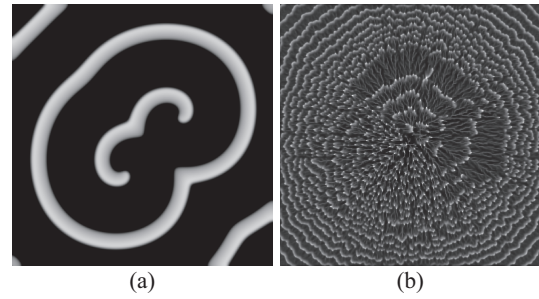


Fig. 2. Numerical simulation of spatial patterns observed in reaction-diffusion systems. Figure (a) shows two spiral cores and propagating waves in the Belousov-Zhabotinsky reaction system [4]. Figure (b) shows signal propagation waves overlaid with a cell density distribution organized in a *Dictyostelium discoideum* [32].

or

$$\mathcal{D}(U_0; D_1, t) - \mathcal{D}(U_0; D_2, t), \quad 0 < D_1 < D_2. \quad (4)$$

Figure 1(b) shows the difference of two solutions $\mathcal{D}(U_0; D, 1.0) - \mathcal{D}(U_0; D, 10.0)$; a zero-crossing point is indeed located at the edge position in the initial condition U_0 . Since an edge is defined as an inflection point, the Laplacian operator in the diffusion equation detects edges contained in an initial condition as zero-crossing points.

A Gaussian filter or a diffusion equation unfortunately removes precise structures in an image intensity distribution. In order to preserve edges of meaningful precise structures such as sharp corners, Perona and Malik [30] and Black et al. [31] proposed edge detection algorithms utilizing anisotropic diffusion equations.

B. Reaction-diffusion equations

A reaction-diffusion system is generally described with a set of time-evolving partial differential equations. Each equation consists of a diffusion equation coupled with a reaction term. Most typical form of a reaction-diffusion system is described with a pair of reaction-diffusion equations having an activator variable u and an inhibitor variable v , as follows:

$$\partial_t u = D_u \nabla^2 u + f(u, v), \quad (5)$$

$$\partial_t v = D_v \nabla^2 v + g(u, v), \quad (6)$$

in which $f(u, v)$ and $g(u, v)$ are reaction terms; the variables u and v are defined in space \mathbf{x} and at time t ; D_u and D_v are diffusion coefficients. Initial conditions for u and v are $u(\mathbf{x}, t = 0.0) = U_0(\mathbf{x})$ and $v(\mathbf{x}, t = 0.0) = V_0(\mathbf{x})$.

The Belousov-Zhabotinsky reaction exhibits non-linear reaction on chemical substances; the Oregonator model describes the non-linear reaction. Since the chemical substances induce chemical reaction and simultaneously diffuse, the chemical reaction system on two-dimensional space self-organizes spatio-temporal patterns of such as propagating target and spiral waves. Keener and Tyson proposed a model of reaction-diffusion equations with the Oregonator model [4]. Figure 2(a) shows a spatial pattern numerically simulated with the reaction-diffusion equations proposed by Keener and Tyson.

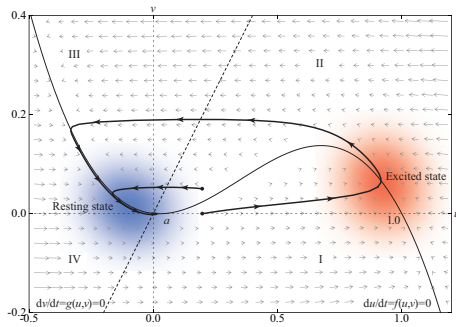


Fig. 3. Phase plot of the FitzHugh-Nagumo ordinary differential equations: $du/dt = f(u, v) = [u(u-a)(1-u) - v]/\varepsilon$ and $dv/dt = g(u, v) = u - bv$. The intersection of $du/dt = 0$ depicted by a solid line and $dv/dt = 0$ depicted by a dotted line is a stable steady state for the equations. An excited state refers to an area having a large value of u , and a resting state refers to the intersection and its neighboring area. Under a positive small constant $0 < \varepsilon \ll 1$, depending on du/dt and dv/dt , a solution (u, v) traces the trajectories denoted by arrows as time proceeds. The signs of du/dt and dv/dt are as follows: $du/dt > 0$ and $dv/dt > 0$ in the area I, $du/dt < 0$ and $dv/dt > 0$ in the area II, $du/dt < 0$ and $dv/dt < 0$ in the area III, and $du/dt > 0$ and $dv/dt < 0$ in the area IV.

There is another interesting reaction-diffusion system in a biological system, the Dictyostelium discoideum, which is a kind of amoeba. A signal propagation process observed in the system is also described with a set of reaction-diffusion equations. However, an interesting point in the system is that a cell density distribution dynamically modulates a reaction term in the equations. The system also self-organizes spatio-temporal patterns, such as, target and spiral waves; at the same time, their propagation speed, shape and oscillation period change dynamically. The dynamical changes are explained with the reaction term depending on the cell density distribution [32]. That is, the reaction term $f(\dots)$ depends not only on the two variables u and v , but also on a variable of cell density, of which a distribution dynamically changes during cell movement. Figure 2(b) shows a numerical result of a cell density distribution and a signal distribution in two-dimensional space.

The system of the FitzHugh-Nagumo reaction-diffusion equations is one of the most popular reaction-diffusion systems. The FitzHugh-Nagumo reaction-diffusion equations simulate an active pulse transmission process along a nerve axon [33], [34]. The equations have reaction terms $f(u, v)$ and $g(u, v)$, as follows:

$$f(u, v) = [u(u-a)(1-u) - v]/\varepsilon, \quad (7)$$

$$g(u, v) = u - bv, \quad (8)$$

in which a and b are constants and ε is a positive small constant ($0 < \varepsilon \ll 1$).

In order to understand the reaction terms $f(u, v)$ and $g(u, v)$ of Eqs. (7) and (8), we show examples of solution trajectories computed for the ordinary differential equations $du/dt = f(u, v)$ and $dv/dt = g(u, v)$ in Fig. 3. Since the intersection of $du/dt = 0$ and $dv/dt = 0$ is a stable steady state, a solution (u, v) finally converges to the state from any initial point. Even if the solution once has a large value of u , it traces a global trajectory and finally converges to the

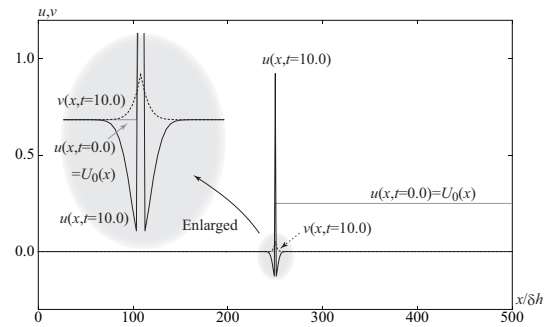


Fig. 4. One-dimensional result for a discretized version of the FitzHugh-Nagumo reaction-diffusion equations. A finite difference in space x is δh . An initial condition for $u(x, t = 0.0) = U_0(x)$ is a step-wise distribution; an initial condition for $v(x, t = 0.0)$ is 0.0 in the whole space. A pulse was organized in the center of the space, as shown in $u(x, t = 10.0)$.

stable steady state. An excited state refers to an area having a large value of u ; a resting state refers to the origin and its neighboring area, as shown in Fig. 3.

In the reaction terms of Eqs. (7) and (8), the parameter a works as a threshold level for an initial condition. Let us consider an initial condition of the solution $(u, v) = (a + \delta, 0)$. If $\delta > 0$, the solution (u, v) enters an excited state; if $\delta < 0$, it immediately enters a resting state. Thus, the system of the ordinary differential equations $du/dt = f(u, v)$ and $dv/dt = g(u, v)$ has the function of dividing its initial condition into two different states: the excited state and the resting state. This brings the primitive idea of detecting edges with the fixed threshold level a for an image intensity distribution.

C. A discretized version of a reaction-diffusion system and its numerical computation

For a stable stationary solution of edges, the reaction-diffusion system must be sparsely discretized under the strong inhibition $D_u \ll D_v$ [22], [24]. Although the earliest work done by Kuhnert et al. shows impressive results of edge detection and segmentation with a real chemical reaction system [16], it does not provide stable results, which are necessary for a realistic algorithm of image processing. In comparison to that, Ebihara et al. [22] and Kurata et al. [24] have found that the discretized version of the reaction-diffusion system under the strong inhibition brings stable stationary results of edge detection and segmentation.

The strong inhibition $D_u \ll D_v$ required for our previous reaction-diffusion algorithm of edge detection is somewhat similar to the Turing scenario [8], [9], to the long-range inhibition causing the Mach bands effect [14] and to the long-range inhibition of the difference of two Gaussian filters [27]. Thus, these similarities furthermore inspire us to develop reaction-diffusion algorithms. It would be interesting, if reaction-diffusion systems modeling pattern formation processes, in particular, biological pattern formation processes in the Turing scenario are also helpful in modeling visual functions required in pattern recognition processes. In addition, the discreteness is also interesting from a biological point of view.

Figure 4 shows an example of an edge detection result in one-dimensional space $x \in \mathbf{R}^1$. A discretized version of the

FitzHugh-Nagumo reaction-diffusion equations self-organizes a pulse at an edge position in a step-wise distribution provided as an initial condition $U_0(x)$. An initial condition for V_0 is $V_0 = 0.0$ in its whole space. The pulse appears after finite duration of time. By searching a distribution of u for a pulse, we can find an edge position for the distribution of the initial condition U_0 .

The following describes discretization of a reaction-diffusion equation and a numerical computation scheme in two-dimensional space $\mathbf{x} = (x, y) \in \mathbf{R}^2$. Space variables (x, y) and a time variable t are discretized with finite differences: δh in space and δt in time, as follows:

$$i = [x/\delta h], j = [y/\delta h] \text{ and } k = [t/\delta t],$$

in which i, j and k are the index number of discretely expressed space and time, and $[\cdot]$ denotes the floor function. Then, for example, the relation between the variable $u(x, y, t)$ and its discrete expression $u_{i,j}^k$ becomes

$$u_{i,j}^k = u(i\delta h, j\delta h, k\delta t). \quad (9)$$

The next equations $\Delta_t u$, $\Delta_{xx} u$ and $\Delta_{yy} u$ respectively describe the discretized versions of $\partial u/\partial t$, $\partial^2 u/\partial x^2$ and $\partial^2 u/\partial y^2$, as follows:

$$\begin{aligned} \Delta_t u &= \frac{u_{i,j}^{k+1} - u_{i,j}^k}{\delta t}, \\ \Delta_{xx} u &= r \frac{u_{i+1,j}^{k+1} - 2u_{i,j}^{k+1} + u_{i-1,j}^{k+1}}{\delta h^2} \\ &\quad + (1-r) \frac{u_{i+1,j}^k - 2u_{i,j}^k + u_{i-1,j}^k}{\delta h^2}, \\ \Delta_{yy} u &= r \frac{u_{i,j+1}^{k+1} - 2u_{i,j}^{k+1} + u_{i,j-1}^{k+1}}{\delta h^2} \\ &\quad + (1-r) \frac{u_{i,j+1}^k - 2u_{i,j}^k + u_{i,j-1}^k}{\delta h^2}, \end{aligned} \quad (10)$$

in which r is fixed at $r = 0.5$ (the Crank-Nicolson scheme [35]). With Eqs. (9) and (10), the reaction-diffusion equation of Eq. (5) becomes a discretized version of a linear equation:

$$\begin{aligned} -C_r u_{i,j-1}^{k+1} - C_r u_{i-1,j}^{k+1} + (1+4C_r) u_{i,j}^{k+1} \\ - C_r u_{i+1,j}^{k+1} - C_r u_{i,j+1}^{k+1} = b_{i,j}^k, \end{aligned} \quad (11)$$

in which $C_r = r D_u \delta t / \delta h^2$; $b_{i,j}^k$ is

$$\begin{aligned} b_{i,j}^k = C_1 u_{i,j-1}^k + C_1 u_{i-1,j}^k + (1-4C_1) u_{i,j}^k \\ + C_1 u_{i+1,j}^k + C_1 u_{i,j+1}^k + \delta t f(u_{i,j}^k, v_{i,j}^k), \end{aligned} \quad (12)$$

in which $C_1 = (1-r) D_u \delta t / \delta h^2$. In image processing, we usually consider a discrete rectangular space denoted by $i = 0, 1, \dots, I-1$ and $j = 0, 1, \dots, J-1$, in which $I \times J$ (pixels) denotes an image size of the space. If the Neumann boundary condition governs the four sides of the rectangular space, it is expressed for the variable u as

$$\begin{aligned} u_{i,-1}^k = u_{i,0}^k, u_{i,J-1}^k = u_{i,J}^k, i = 0, 1, \dots, I-1, \\ u_{-1,j}^k = u_{0,j}^k, u_{I-1,j}^k = u_{I,j}^k, j = 0, 1, \dots, J-1. \end{aligned} \quad (13)$$

For given initial conditions $(u_{i,j}^{k=0}, v_{i,j}^{k=0}) = (U_{0,i,j}, V_{0,i,j})$ and the boundary conditions of Eq. (13), we compute $u_{i,j}^{k=1}$ by

solving a set of linear equations described by Eq. (11) with Eq. (12). Thus, by iteratively computing $u_{i,j}^{k+1}$ from $u_{i,j}^k$, we can obtain a time-evolving solution (u, v) . The Gauss-Seidel scheme [35], for example, provides a solution for a set of linear equations.

Chen and Wang also proposed a segmentation algorithm utilizing the locally excitatory globally inhibitory oscillator network named LEGION, which spatially couples the FitzHugh-Nagumo ordinary differential equations controlled by a global inhibitor [36].

III. REACTION-DIFFUSION ALGORITHM FOR EDGE DETECTION

As described in the above section II-C, a single pair of the discretized version of the FitzHugh-Nagumo reaction-diffusion Eqs. (5)~(8) has a function of detecting edges for a binary image. The version firstly divides an initial condition U_0 into a brighter or darker level with a threshold level a . Then, the version self-organizes a pulse at the boundary between the two levels. Thus, when utilizing the single pair with the fixed parameter a , we cannot expect edge detection for a gray level image. Figures 5(a) and 5(b) show a situation in which the discretized version organized one pulse at one of the two edge positions for a step-wise distribution having three different levels. In the situation, we fixed the threshold level a at $a = 0.05$ between the two intensity levels: the darkest one ($U_0 = 0.00$) and the middle one ($U_0 = 0.10$).

We confirm how a single pair of a discretized version of the FitzHugh-Nagumo reaction-diffusion equations having the parameter $a = a(\mathbf{x})$ [23] works for an initial condition U_0 of a step-wise distribution. In contrast to the fixed parameter a , we consider a spatial distribution $a(\mathbf{x})$. When $a(\mathbf{x}) = U_0(\mathbf{x})$, the system does not organize any pulse in $u(\mathbf{x}, t)$. When we provide a distribution diffused from $U_0(\mathbf{x})$ to $a(\mathbf{x})$, we obtain pulses. The diffused distribution intersects its original distribution U_0 at its inflection point, as shown in Fig. 1(a). Since the parameter a works as a threshold level for an initial condition, the difference between the diffused distribution $a(\mathbf{x}) = \mathcal{D}(U_0; D, T)$ and the original one U_0 causes a pulse at the edge position. Figures 5(c) and 5(d) show two examples of the situation in one-dimensional space $x \in \mathbf{R}^1$; a weakly diffused distribution or a strongly diffused one was provided for $a(x)$. The single pair organizes pulses not only at the true edge positions, but also false pulses in neighboring area of the true pulses. Spacing between the true pulse and its paired false pulse depends on how much the distribution $a(x)$ is diffused from $U_0(x)$, that is, on the parameters D and T in $\mathcal{D}(U_0; D, T)$. This is clearly recognizable by the comparison of the two examples shown in Figs. 5(c) and 5(d). This is because the system organizes pulses at both ends of an area satisfying the condition $U_0(x) > a(x)$; the stronger the diffusion becomes, the larger the area becomes. We need to eliminate the false pulses standing at the false edge positions from the distribution $u(x, t)$ of the reaction-diffusion equations.

Here, we propose a reaction-diffusion algorithm detecting edges from a gray level image. The algorithm consists of

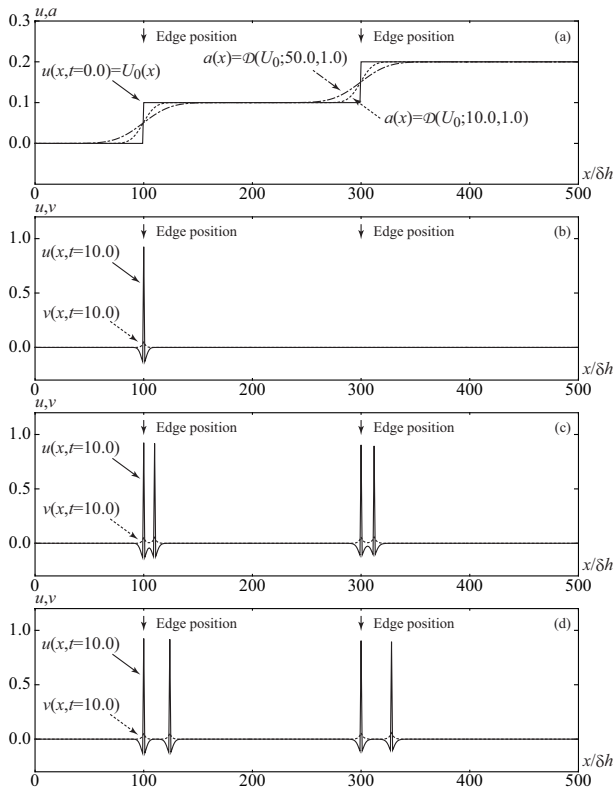


Fig. 5. One-dimensional results obtained by a single pair of a discretized version of the FitzHugh-Nagumo reaction-diffusion equations, for which a step-wise distribution having three different levels was provided as its initial condition $u(x, t = 0.0) = U_0(x)$. An initial condition for $v(x, t = 0.0)$ was zero. Figure (a) shows the step-wise distribution $U_0(x)$ indicated by a solid line and its diffused distributions of $\mathcal{D}(U_0; 50.0, 1.0)$ indicated by a dotted broken line and $\mathcal{D}(U_0; 10.0, 1.0)$ indicated by a dotted line. Figure (b) shows a result obtained by the discretized version with the fixed value $a = 0.05$. Figure (c) shows a result obtained by the discretized version with the variable $a(x) = \mathcal{D}(U_0; 10.0, 1.0)$. Figure (d) shows a result obtained by the discretized version with the variable $a(x) = \mathcal{D}(U_0; 50.0, 1.0)$. In each of (b), (c) and (d), a solid line indicates $u(x, t = 10.0)$ and a dotted line indicates $v(x, t = 10.0)$. Parameter settings utilized here were $b = 1.0$, $\varepsilon = 1.0 \times 10^{-3}$, $D_u = 1.0$, $D_v = 5.0$, $\delta h = 0.5$, $\delta t = 1.0 \times 10^{-4}$.

two pairs of a discretized version of the FitzHugh-Nagumo reaction-diffusion equations having variables $u_c(x, t)$, $v_c(x, t)$ and a source term, as follows:

$$\partial_t u_0 = D_u \nabla^2 u_0 + f(u_0, v_0, a_0) + \partial_t u_1 \Theta(-\partial_t u_1), \quad (14)$$

$$\partial_t u_1 = D_u \nabla^2 u_1 + f(u_1, v_1, a_1), \quad (15)$$

$$\partial_t v_c = D_v \nabla^2 v_c + g(u_c, v_c), \quad (16)$$

$$a_c = \mathcal{D}(U_0; D_{a_c}, T), \quad D_{a_0} < D_{a_1}, \quad (17)$$

in which the function $\Theta(s)$ gives 1, if $s \geq 0$, and otherwise 0; $c = 0, 1$ is an index number of the two pairs. Although $f(\cdot, \cdot, \cdot)$ and $g(\cdot, \cdot, \cdot)$ are the same as Eqs. (7) and (8), $a_c(x)$ is variable in space x . The diffusion coefficients D_u and D_v must satisfy the condition $D_u \ll D_v$, which is the same as that imposed on the previous reaction-diffusion algorithms [21], [22], [23], [24]. The algorithm takes a gray level image as an initial condition U_0 provided for both u_0 and u_1 ; an initial condition V_0 for both v_0 and v_1 is zero. Equation (17) states that the spatial distributions a_c , $c = 0, 1$ take diffused U_0 , and a_1 must be diffused more than a_0 .

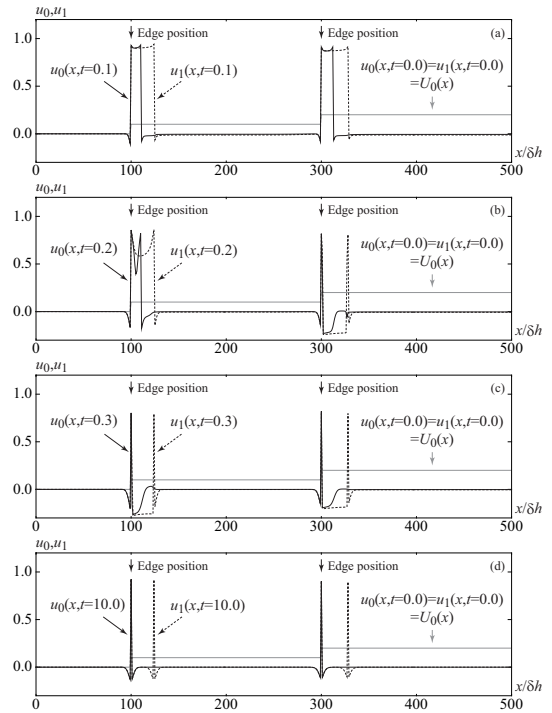


Fig. 6. Temporal developments of activator variables during an edge detection process for a step-wise distribution. Figures (a), (b), (c) and (d) show one-dimensional distributions of u_0 and u_1 at time instances: $t = 0.1, 0.2, 0.3, 10.0$ as well as their initial conditions $u_0(x, t = 0.0) = u_1(x, t = 0.0) = U_0(x)$. Parameter settings utilized here were $D_u = 1.0$, $D_v = 5.0$, $b = 1.0$, $\varepsilon = 1.0 \times 10^{-3}$, $\delta h = 0.5$, $\delta t = 1.0 \times 10^{-4}$. One-dimensional distributions of a_0 and a_1 were $a_0 = \mathcal{D}(U_0; 10.0, 1.0)$ and $a_1 = \mathcal{D}(U_0; 50.0, 1.0)$.

In the proposed algorithm, the term $\partial_t u_1 \Theta(-\partial_t u_1)$ in Eq. (14) eliminates false pulses organized in u_0 . After preparing the two distributions a_0 and a_1 according to Eq. (17), at $t = 0.0$ the algorithm initiates computation of discretized versions of Eqs. (14)~(16) for an initial condition (U_0, V_0) . Figure 6 shows an example of how the proposed algorithm works for a step-wise distribution having three different levels in a one-dimensional space. Firstly, the two sets of the solutions (u_0, v_0) and (u_1, v_1) move towards an excited state of the FitzHugh-Nagumo equations in the area of $a_c < U_0$, $c = 0, 1$. Next, the two solutions except the true edge positions and false edge positions return to a resting state from the excited state (see also the global trajectory show in Fig. 3). In particular, let us focus on the solution (u_1, v_1) in the area between the true edge position and the false edge position. When the solution (u_1, v_1) returns to the resting state, its temporal change $\partial_t u_1$ becomes negative in the area. Since the false pulse in u_0 is located between the true edge position and the false edge position in u_1 [see also Figs. 5(c) and 5(d)], the false pulse in u_0 is affected by the negative external stimulus $\partial_t u_1$ in Eq. (14). As the result, the false pulse is eliminated in u_0 ; the true pulses in u_0 and u_1 and the false pulse in u_1 survive, as shown in Fig. 6(d). Thus, after the discretized version converges, the algorithm detects edges by searching u_0 for pulses. Finally, an edge map $\mathcal{M}(t)$ at time t is obtained, as

follows:

$$\mathcal{M}(t) = \{\mathbf{x} | u(\mathbf{x}, t) > \theta\}, \quad (18)$$

in which θ is a threshold level for judgment of an excited state or not, and is fixed at 0.5.

We conclude this section by summarizing the proposed reaction-diffusion algorithm for edge detection. The algorithm consists of the following steps:

Step 1: Let $B(\mathbf{x})$ be a gray level image, which is normalized as $0 \leq B(\mathbf{x}) \leq 1/4$.

Step 2: Prepare initial conditions as $U_0(\mathbf{x}) = B(\mathbf{x})$ and $V_0(\mathbf{x}) = 0$.

Step 3: Prepare distributions of $a_0(\mathbf{x})$ and $a_1(\mathbf{x})$ with Eq. (17).

Step 4: Iteratively compute the discretized version of Eqs. (14)~(16) under the strong inhibition $D_u \ll D_v$. Refer to Section II-C for discretization of the reaction-diffusion equations.

Step 5: Compute an edge map $\mathcal{M}(t)$ with Eq. (18), after enough duration of time.

IV. EXPERIMENTAL RESULTS AND DISCUSSION

This section presents experimental results of edge detection with the proposed reaction-diffusion algorithm and a representative algorithm proposed by Canny [26] for comparison. Performance of the algorithms for artificial images is evaluated with the ground-truth data of edges. Then, there is demonstration on how the algorithms work for real images. Upon these results, we discuss the characteristics of the proposed algorithm, in comparison to the Canny algorithm. Finally, there is confirmation on the convergence of the proposed algorithm for the artificial and real images.

Figure 7 shows results of edge detection for artificial images. In order to confirm the basic performance of the previous reaction-diffusion algorithm having a fixed parameter a , we applied the algorithm to a binary image of Fig. 7(a). In addition, we applied the proposed reaction-diffusion algorithm and the Canny algorithm to a gray level image of Fig. 7(b). Figure 7(c) shows the ground-truth data of edges contained in the binary and gray level images.

Let us focus on the edge detection result obtained with the previous reaction-diffusion algorithm having a fixed parameter value a [see Fig. 7(d)]. Although the algorithm detected edges almost correctly for the binary image shown in Fig. 7(a), it failed to detect edges of tiny letters contained in the cells A3, B4, C1 and D2 in Fig. 7(d). In particular, the algorithm completely failed to detect edges of letters contained in the cell B4. In the fails of the cells A3, B4, C1 and D2, we can find a common situation; white background regions surround tiny black regions of letters. We can also find the situation partly in the cell D4; white regions surround corners of small black squares regularly placed and the algorithm failed to detect edges at the corners. The white regions cause reaction-diffusion waves, which slightly propagate into the tiny black regions and diffuse. Thus, the tiny black regions are removed out and no waves indicating edges survived. In comparison to the situation, the algorithm successfully detected edges of tiny white regions surrounded by black regions, for example,

TABLE I

Quantitative evaluations of edge detection algorithms. The error measure E_t (%) denotes a percentage of undetected edges over the number of the true edges $|\mathcal{M}_t|$ [see Eq. (19)]. The error measure E_o (%) denotes a percentage of incorrectly detected edges over the number of detected edges $|\mathcal{M}_o|$ [see Eq. (20)]. Evaluated algorithms are the reaction-diffusion algorithm previously proposed with a fixed parameter a (RDA-fixed), that proposed in the present paper with a variable $a(\mathbf{x})$ (RDA-variable), and an edge detection algorithm proposed by Canny [26] (Canny). The result for the algorithm RDA-fixed was obtained for an artificial binary image [Fig. 7(a)], the results for the algorithm RDA-variable and Canny were obtained for an artificial gray level image [Fig. 7(b)]. Refer to Fig. 7(c) for the ground-truth data of edges.

Algorithm	\mathcal{M}_o	$ \mathcal{M}_t $	E_t (%)	$ \mathcal{M}_o $	E_o (%)
RDA-fixed	Fig. 7(d)		30.62	13,825	10.39
RDA-variable	Fig. 7(e)	20,732	23.07	16,877	11.44
Canny	Fig. 7(f)		8.20	21,069	8.08

as shown in the cells B3, C2 and D1. In our supplementary experiments, which is not shown in the present paper, the algorithm successfully detected edges in the cells A3, B4, C1 and D2 from its black-and-white inverted binary image. This is also additional evidence with which we can explain the reason why the tiny black regions are undetected and the tiny white regions are detected. In order to improve the previous algorithm for tiny black regions, we need to utilize both an original binary image and its black-and-white inverted binary image.

Next, let us focus on edge detection results obtained with the proposed reaction-diffusion algorithm and the Canny algorithm [26]. Figures 7(e) and 7(f) show the results. In the cells A3, B4, C1 and D2, the proposed algorithm also failed to detect edges in relatively dark tiny regions, such as small letters; this is the similar situation to the results of Fig. 7(d). When comparing the result of the proposed algorithm with that of the Canny algorithm, we can state that the Canny algorithm provided almost correct results of edge detection. However, when focusing on several details in the edge detection results, we can find some artifacts in the result of the Canny algorithm, in particular, at cross sections and at corners. For example, as shown in the cells of D3, on the one hand, the proposed algorithm detected correctly at corners of the triangle; on the other hand, the Canny algorithm detected slightly rounded edges at the corners.

In order to confirm overall performance of the edge detection algorithms, we evaluated the results shown in Figs. 7(d), 7(e) and 7(f) by comparing each of obtained edge maps with the ground-truth data of Fig. 7(c). The next error measures E_t and E_o evaluate quantitative performance of an edge detection algorithm, as follows:

$$E_t = \frac{1}{|\mathcal{M}_t|} |\mathcal{M}_t \cap \overline{\mathcal{M}_o}| \times 100 \quad (\%), \quad (19)$$

$$E_o = \frac{1}{|\mathcal{M}_o|} |\mathcal{M}_o \cap \overline{\mathcal{M}_t}| \times 100 \quad (\%), \quad (20)$$

in which \mathcal{M}_t is the ground-truth data of an edge map and \mathcal{M}_o is an obtained edge map; $|\mathcal{M}_t|$ is the number of the true edges in \mathcal{M}_t and $|\mathcal{M}_o|$ is the number of detected edges in \mathcal{M}_o . Thus, Eq. (19) denotes the percentage of the number of undetected edges over the number of the true edges; Eq. (20)

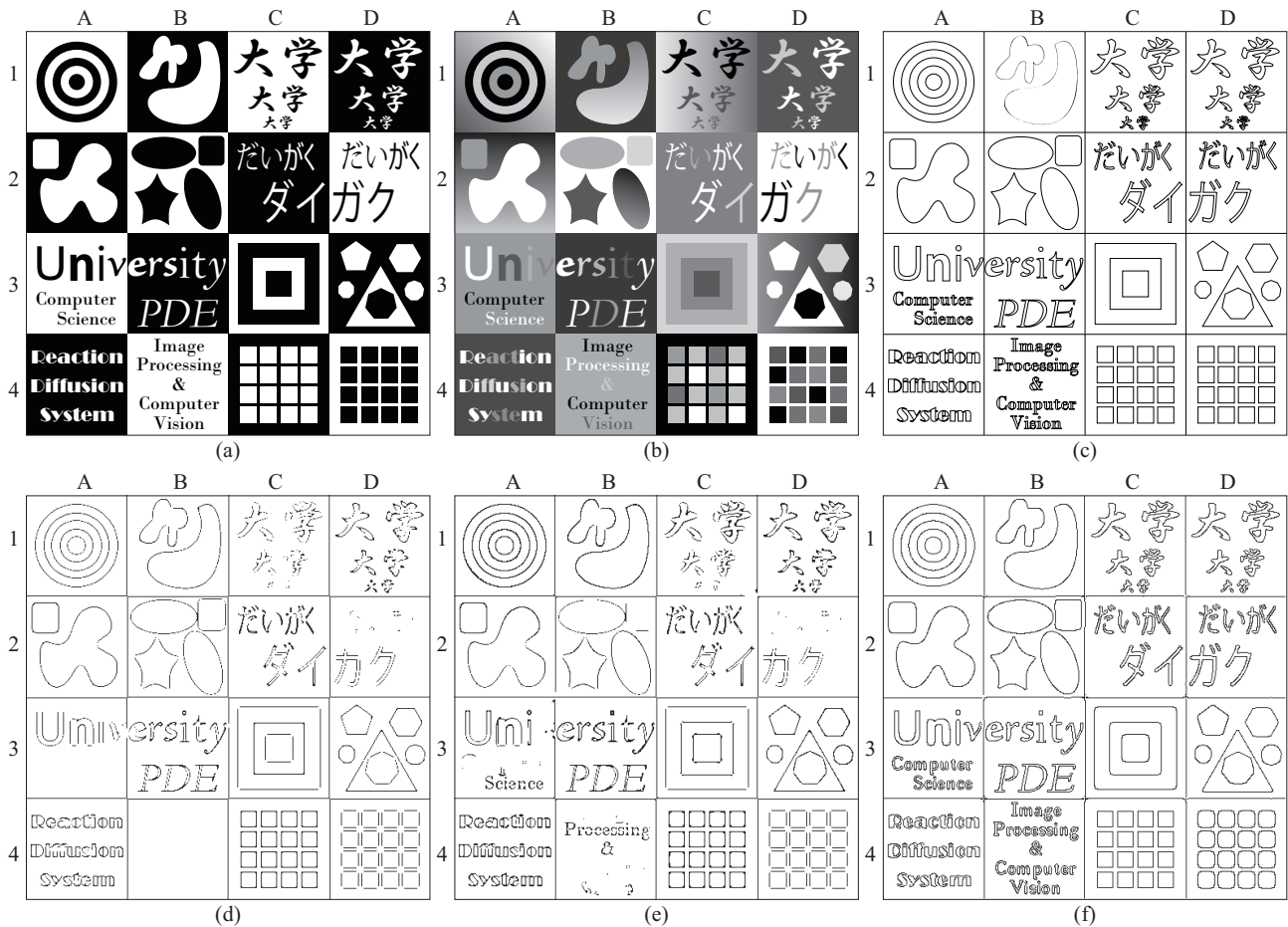


Fig. 7. Edge detection results for artificial images. Figures (a) and (b) show a binary image and a gray level image with a size of 500×500 (pixels). Figure (c) shows the ground-truth data of edges contained in (a) and (b); black dots and lines indicate the edges. Figure (d) shows an edge detection result obtained for the binary image (a) with the previous edge detection algorithm, which utilizes a single pair of a discretized version of the FitzHugh-Nagumo reaction-diffusion equations [21], [22], [24]. The parameter settings were $D_u = 1.0$, $D_v = 5.0$, $a = 0.05$, $b = 1.0$, $\varepsilon = 1.0 \times 10^{-3}$, $\delta h = 0.5$, $\delta t = 1.0 \times 10^{-4}$. Figure (e) shows an edge detection result obtained for the gray level image (b) with the proposed reaction-diffusion algorithm. The parameter settings were $D_u = 1.0$, $D_v = 5.0$, $b = 1.0$, $\varepsilon = 1.0 \times 10^{-3}$, $D_{a_0} = 10.0$, $D_{a_1} = 50.0$, $T = 1.0$, $\delta h = 0.5$, $\delta t = 1.0 \times 10^{-4}$. Figure (f) shows an edge detection result obtained for the gray level image (b) with the Canny algorithm [26]. The parameter settings were $\sigma = 0.80$, the lower threshold level=0.05 and the higher threshold level=0.15. The images and the results have 16 cells, each of which is named with a row number: 1, 2, 3, 4 and a column letter: A, B, C, D. For example, the left top cell is named A1. Refer to Table I for quantitative evaluations of the results (d), (e) and (f).

denotes the percentage of the number of incorrectly detected edges over the number of detected edges. In both measures, a smaller value E_t or E_o with a larger number $|\mathcal{M}_t|$ or $|\mathcal{M}_o|$ indicates better performance. Table I shows the results of the quantitative evaluation. The Canny algorithm almost correctly detected edges contained in the ground-truth data of the edge map ($E_t = 8.20\%$); edges detected by the algorithm are almost correct ($E_o = 8.08\%$). In comparison, however edges detected by the reaction-diffusion algorithms are almost correct ($E_o = 10.39\%$ on RDA-fixed and $E_o = 11.44\%$ on RDA-variable), there were many undetected edges ($E_t = 30.62\%$ on RDA-fixed and $E_t = 23.07\%$ on RDA-variable). We believe that the problem of many undetected edges should be partly solvable with further development done for the reaction-diffusion algorithm with a black-and-white inverted image.

Furthermore, we tested the algorithms for real gray level images. Figure 8 shows results of edge detection with the proposed reaction-diffusion algorithm and the Canny algorithm. From comparison between each of the results obtained with

the two algorithms, we can recognize a significant difference. The Canny algorithm detected continuous edges, which are due to the final step merging small edges or disjointed edges in the algorithm. In comparison, the edge maps obtained with the proposed algorithm contain small uncertain edges like randomly distributed noise. In the reaction-diffusion algorithm, we also need to employ such an algorithm merging neighboring disjointed edges, if we impose a continuity condition on detected edges.

Let us focus on the image of Fig. 8(d), which has highly defocused objects in the background and their shadow on the wall, in addition to the focused object of a videocamera. It is believed that the human visual system integrates monocular contour information into the stereo depth perception [38]. In this context, we believe that defocused edges are also helpful to stereo disparity detection. Thus, we need to evaluate edge strength indicating how rapidly an intensity distribution changes across an edge [39], for more psychologically plausible visual information processing. This is an interesting topic

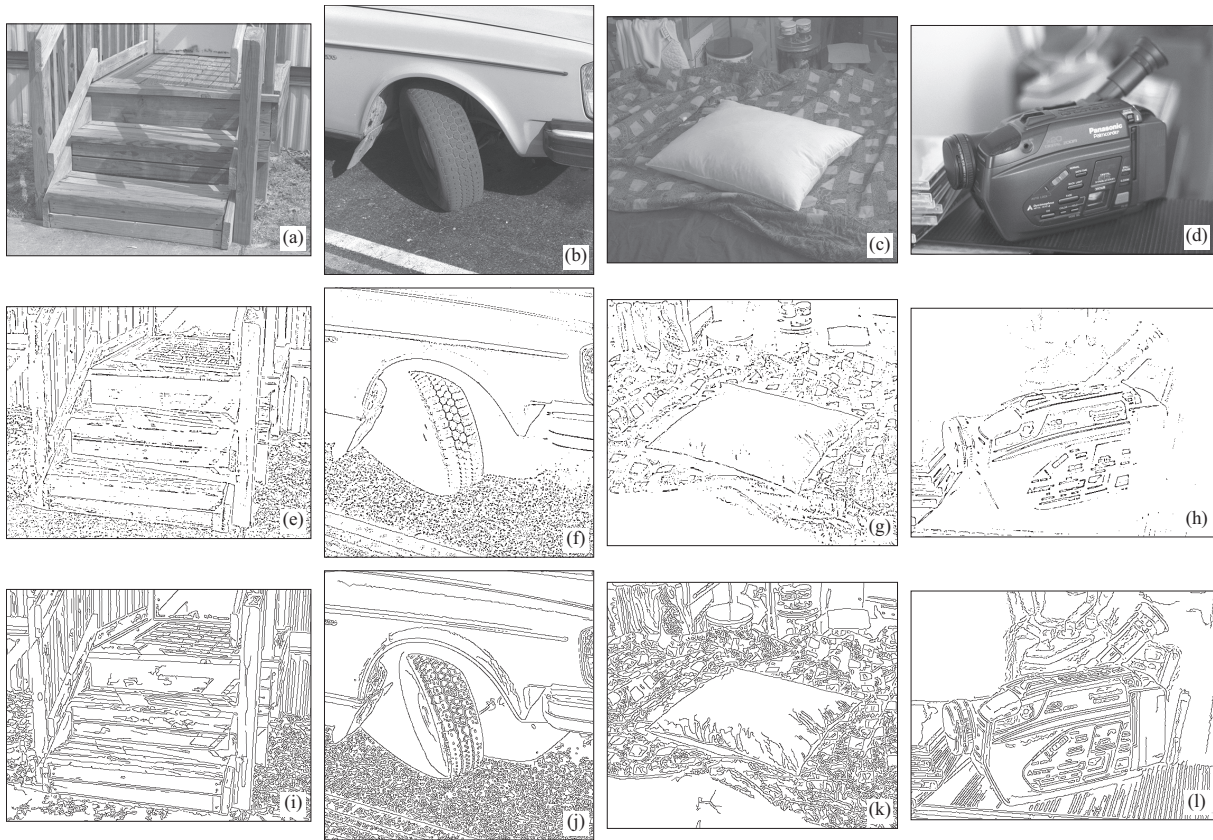


Fig. 8. Edge detection results for real images. The real images are (a) Stairs [579 × 441 (pixels)], (b) Tire [512 × 512 (pixels)], (c) Pillow [552 × 468 (pixels)] and (d) Videocamera [577 × 435 (pixels)]. Figures (e)~(h) show edge detection results obtained with the proposed reaction-diffusion algorithm. The parameter settings were $D_u = 1.0$, $D_v = 5.0$, $D_{a_0} = 10.0$, $D_{a_1} = 50.0$, $b = 1.0$, $\varepsilon = 1.0 \times 10^{-3}$, $\delta h = 0.5$, $\delta t = 1.0 \times 10^{-4}$. Figures (i)~(l) show edge detection results obtained with the Canny algorithm [26]. The parameter settings were $\sigma = 1.20$, the lower threshold level=0.20 and the higher threshold level=0.60. The real images are provided on the website "Edge Detector Comparison" (http://marathon.csee.usf.edu/edge/edge_detection.html) by Heath et al. [37].

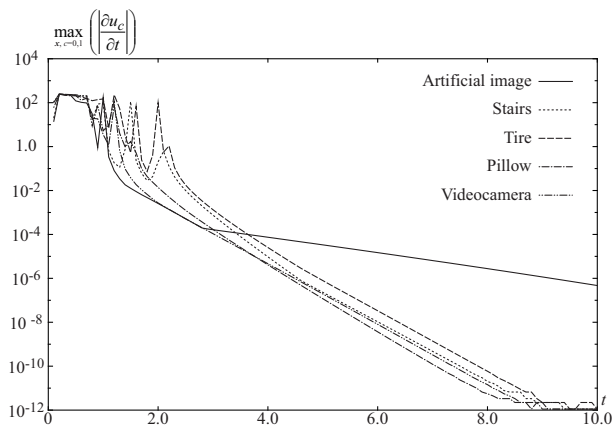


Fig. 9. Convergence of the proposed reaction-diffusion algorithm. Temporal changes of $\max_{x,c=0,1}(|\partial u_c/\partial t|)$ measured for an artificial image shown in Fig. 7(b) and for real images: Stairs, Tire, Pillow and Videocamera shown in Figs. 8(a)~(d).

and future research work required for the reaction-diffusion algorithm of edge detection.

Finally, we confirmed convergence of the proposed reaction-diffusion algorithm for the artificial and real images uti-

lized above. The algorithm iteratively solves linear equations derived at every time instance from time-evolving partial differential Eqs. (14), (15) and (16) having variables u_c and v_c . If the temporal changes $\partial u_c/\partial t$, $c = 0, 1$ converge to zero as time proceeds, we can state that the algorithm converges. Thus, during the edge detection processes reported above we measured temporal changes of $\max(|\partial u_c/\partial t|)$ for any x and $c = 0, 1$. Figure 9 shows the temporal changes measured for the images. The results of the changes show that the proposed algorithm indeed converges. We utilized the Gauss-Seidel scheme for solving the linear equations derived at every time instance. The scheme is an iterative method and judges its convergence with a small value, which was 1.0×10^{-16} in the present experiments. In addition, the finite difference in time was $\delta t = 1.0 \times 10^{-4}$. Thus, the temporal change $\max_{x,c=0,1}(|\partial u_c/\partial t|)$ should achieve the minimum at the order of 10^{-12} . According to Fig. 9, we can state that the proposed algorithm completely converged for the real images at around $t = 9$. Although the algorithm did not achieve the minimum value for the artificial image, it was indeed converging.

V. CONCLUSION

This paper presented a quick review of reaction-diffusion systems exhibiting pattern formation processes and proposed a reaction-diffusion algorithm detecting edges from gray level images. Pattern formation processes are found in several natural systems including biological and chemical systems. One of the typical chemical systems is the Belousov-Zhabotinsky reaction system [1], [2], which is described with two diffusion processes coupled with non-linear chemical reaction terms, that is, reaction-diffusion equations having activator and inhibitor variables [4]. Another one is the biological system: Dictyostelium discoideum, of which the pattern formation process of signaling waves is also described with reaction-diffusion equations [32]. The interesting point in the biological system is that a reaction term of the equations is dynamically modulated by a cell density distribution. These two previous reaction-diffusion systems highly inspired us to model visual functions and to develop computer algorithms utilizing reaction-diffusion equations for image processing and computer vision research.

We have two previous reaction-diffusion algorithms designed for edge detection. However, one of the previous algorithms utilizes a single pair of a discretized version of the FitzHugh-Nagumo reaction-diffusion equations; it is not applicable to gray level images [21], [22], [24]. The other previous algorithm utilizes multiple pairs; each pair is coupled with an additional diffusion equation [23]. Thus, it needs much computation time for solving the multiple pairs for a gray level image. The algorithm proposed here utilizes two pairs; each pair has a parameter of a threshold level, which is not fixed at a constant value, but modulated with a diffused gray level image. The proposed algorithm utilizing the two pairs requires less computation time, in comparison to the previous algorithm utilizing the multiple pairs. The idea of coupling the two pairs originated in the mechanism of the dynamical modulation by the cell density distribution in the biological system [32]. On the reaction-diffusion algorithms including the proposed one and the previous ones, we imposed the strong inhibition inspired by stationary pattern formation processes observed in chemical and biological systems; this is the original point in our algorithms.

We tested performance of the reaction-diffusion algorithms and the Canny algorithm [26] by applying them to artificial and real images. As the result, we confirmed that the proposed algorithm is indeed applicable to gray level images. However, the proposed algorithm did not achieve the performance of the Canny algorithm, which is known as one of representative edge detection algorithms. By comparing the edge detection results obtained with the two algorithms, we qualitatively confirmed that the proposed algorithm can detect edges around sharp corners, for example, around corners of a triangle, more correctly in comparison with the Canny algorithm. This is a feature point in the proposed reaction-diffusion algorithm. We believe that the strong inhibition is particularly important at the corners. The Canny algorithm is better than the proposed algorithm in overall quantitative performance measures.

From edge detection results obtained for a real image, we

recognized the following future research work. That is, we need to evaluate edge strength as well as to detect edge positions. Real images have areas of highly defocused objects in their background or foreground. The defocused objects have diffused edges or weak edges, across which image intensity distributions change gradually. We believe that the edge strength information is helpful for a stereo vision system and other visual functions. Thus, we need to develop the reaction-diffusion algorithm for detecting edges and their strength, for which we have already tested a novel idea with multiple pairs of a discretized version of reaction-diffusion equations [40]. This is the future research work required for the reaction-diffusion algorithm of edge detection.

REFERENCES

- [1] A. N. Zaikin and A. M. Zhabotinsky, "Concentration wave propagation in two-dimensional liquid-phase self-oscillating system," *Nature*, vol. 225, pp. 535–537, 1970.
- [2] A. M. Zhabotinsky, "A history of chemical oscillations and waves," *Chaos*, vol. 1, pp. 379–386, 1991.
- [3] J. D. Murray, *Mathematical Biology*. Berlin: Springer-Verlag, 1989.
- [4] J. P. Keener and J. J. Tyson, "Spiral waves in the Belousov-Zhabotinskii reaction," *Physica D*, vol. 21, pp. 307–324, 1986.
- [5] V. Castets, E. Dulos, J. Boissonade, and P. De Kepper, "Experimental evidence of a sustained standing Turing-type nonequilibrium chemical pattern," *Physical Review Letters*, vol. 64, pp. 2953–2956, 1990.
- [6] P. De Kepper, V. Castets, E. Dulos, and J. Boissonade, "Turing-type chemical patterns in the chlorite-iodide-malonic acid reaction," *Physica D*, vol. 49, pp. 161–169, 1991.
- [7] A. Nomura, H. Miike, T. Sakurai, and E. Yokoyama, "Numerical experiments on the Turing instability in the Oregonator model," *Journal of the Physical Society of Japan*, vol. 66, pp. 598–606, 1997.
- [8] A. M. Turing, "The chemical basis of morphogenesis," *Philosophical Transactions of the Royal Society of London. Series B, Biological Sciences*, vol. 237, pp. 37–72, 1952.
- [9] A. Gierer and H. Meinhardt, "A theory of biological pattern formation," *Kybernetik*, vol. 12, pp. 30–39, 1972.
- [10] S. Kondo and R. Asai, "A reaction-diffusion wave on the skin of the marine angelfish *Pomacanthus*," *Nature*, vol. 376, pp. 765–768, 1995.
- [11] S. Sick, S. Reinker, J. Timmer, and T. Schlake, "WNT and DKK determine hair follicle spacing through a reaction-diffusion mechanism," *Science*, vol. 314, pp. 1447–1450, 2006.
- [12] E. Mach, "Über die Wirkung der räumlichen Verteilung des Lichtreizes auf die Netzhaut, I." *Sitzungsber. math.-naturw. Kl. Kaiserlichen Akad. Wiss.*, vol. 52, pp. 303–322, 1865.
- [13] H. K. Hartline, H. G. Wagner, and F. Ratliff, "Inhibition in the eye of *Limulus*," *Journal of General Physiology*, vol. 39, pp. 651–673, 1956.
- [14] R. B. Barlow, Jr. and D. A. Quarles, Jr., "Mach bands in the lateral eye of *limulus*," *Journal of General Physiology*, vol. 65, pp. 709–730, 1975.
- [15] L. Kuhnert, "A new optical photochemical memory device in a light sensitive chemical active medium," *Nature*, vol. 319, pp. 393–394, 1986.
- [16] L. Kuhnert, K. I. Agladze, and V. I. Krinsky, "Image processing using light-sensitive chemical waves," *Nature*, vol. 337, pp. 244–247, 1989.
- [17] T. Sakurai, E. Mihaliuk, F. Chirila, and K. Showalter, "Design and control of wave propagation patterns in excitable media," *Science*, vol. 296, pp. 2009–2012, 2002.
- [18] A. Adamatzky, B. D. L. Costello, and T. Asai, *Reaction-Diffusion Computers*. Amsterdam: Elsevier, 2005.
- [19] T. Matsumoto, "A chaotic attractor from Chua's circuit," *IEEE Transactions on Circuits and Systems*, vol. 31, pp. 1055–1058, 1984.
- [20] M. Gómez-Gesteira, V. Pérez-Muñuzuri, L. O. Chua, and V. Pérez-Villar, "Coexistence of excitability, Hopf and Turing modes in a one-dimensional array of nonlinear circuits," *IEEE Transactions on Circuits and Systems – I: Fundamental Theory and Applications*, vol. 42, pp. 672–677, 1995.
- [21] A. Nomura, M. Ichikawa, H. Miike, M. Ebihara, H. Mahara, and T. Sakurai, "Realizing visual functions with the reaction-diffusion mechanism," *Journal of the Physical Society of Japan*, vol. 72, pp. 2385–2395, 2003.

- [22] M. Ebihara, H. Mahara, T. Sakurai, A. Nomura, A. Osa, and H. Miike, "Segmentation and edge detection of noisy image and low contrast image based on a reaction-diffusion model," *The Journal of the Institute of Image Electronics Engineers of Japan*, vol. 32, pp. 378–385, 2003, [in Japanese].
- [23] A. Nomura, M. Ichikawa, R. H. Sianipar, and H. Miike, "Edge detection with reaction-diffusion equations having a local average threshold," *Pattern Recognition and Image Analysis*, vol. 18, pp. 289–299, 2008.
- [24] N. Kurata, H. Kitahata, H. Mahara, A. Nomura, H. Miike, and T. Sakurai, "Stationary pattern formation in a discrete excitable system with strong inhibitory coupling," *Physical Review E*, vol. 79, p. 056203, 2009.
- [25] A. Nomura, M. Ichikawa, and H. Miike, "Reaction-diffusion algorithm for stereo disparity detection," *Machine Vision and Applications*, vol. 20, pp. 175–187, 2009.
- [26] J. Canny, "A computational approach to edge detection," *IEEE Transactions on Pattern Analysis and Machine Intelligence*, vol. 8, pp. 679–698, 1986.
- [27] D. Marr and E. Hildreth, "Theory of edge detection," *Proceedings of the Royal Society of London. Series B, Biological Sciences*, vol. 207, pp. 187–217, 1980.
- [28] J. J. Koenderink, "The structure of images," *Biological Cybernetics*, vol. 50, pp. 363–370, 1984.
- [29] T. Sunayama, M. Ikebe, T. Asai, and Y. Amemiya, "Cellular ν MOS circuits performing edge detection with difference-of-Gaussian filters," *Japanese Journal of Applied Physics*, vol. 39, pp. 2278–2286, 2000.
- [30] P. Perona and J. Malik, "Scale-space and edge detection using anisotropic diffusion," *IEEE Transactions on Pattern Analysis and Machine Intelligence*, vol. 12, pp. 629–639, 1990.
- [31] M. J. Black, G. Sapiro, D. H. Marimont, and D. Heeger, "Robust anisotropic diffusion," *IEEE Transactions on Image Processing*, vol. 7, pp. 421–432, 1998.
- [32] T. Höfer, J. A. Sherratt, and P. K. Maini, "Cellular pattern formation during Dictyostelium aggregation," *Physica D*, vol. 85, pp. 425–444, 1995.
- [33] R. FitzHugh, "Impulses and physiological states in theoretical models of nerve membrane," *Biophysical Journal*, vol. 1, pp. 445–466, 1961.
- [34] J. Nagumo, S. Arimoto, and S. Yoshizawa, "An active pulse transmission line simulating nerve axon," *Proceedings of the IRE*, vol. 50, pp. 2061–2070, 1962.
- [35] C. A. J. Fletcher, *Computational Techniques for Fluid Dynamics 1: Fundamental and General Techniques*. Berlin, Germany: Springer-Verlag, 1991.
- [36] K. Chen and D. Wang, "A dynamically coupled neural oscillator network for image segmentation," *Neural Networks*, vol. 15, pp. 423–439, 2002.
- [37] M. D. Heath, S. Sarkar, T. Sanocki, and K. W. Bowyer, "A robust visual method for assessing the relative performance of edge-detection algorithms," *IEEE Transactions on Pattern Analysis and Machine Intelligence*, vol. 19, pp. 1338–1359, 1997.
- [38] M. Ichikawa, S. Saida, A. Osa, and K. Munechika, "Integration of binocular disparity and monocular cues at near threshold level," *Vision Research*, vol. 43, pp. 2439–2449, 2003.
- [39] J. H. Elder and S. W. Zucker, "Local scale control for edge detection and blur estimation," *IEEE Transactions on Pattern Analysis and Machine Intelligence*, vol. 20, pp. 699–716, 1998.
- [40] A. Nomura, M. Ichikawa, K. Okada, and H. Miike, "Edge strength evaluation with reaction-diffusion systems," in *Proceedings of the 24th International Image and Vision Computing New Zealand Conference*, 2009, pp. 442–447.